Research Article
Hepatic and Biliary Cancer

JOURNAL OF HEPATOLOGY

Clinicopathologic features, tumor immune microenvironment and genomic landscape of Epstein-Barr virus-associated intrahepatic cholangiocarcinoma

Yu-Hua Huang[1,2,†], Chris Zhi-yi Zhang[3,†], Qun-Sheng Huang[1,2,†], Joe Yeong[4,5,6], Fang Wang[1,7], Xia Yang[1,2], Yang-Fan He[1,2], Xiao-Long Zhang[1], Hua Zhang[8], Shi-Lu Chen[1,2], Yin-Li Zheng[1,2], Ru Deng[1,2], Cen-Shan Lin[1,2], Ming-Ming Yang[1,2], Yan Li[1,2], Chen Jiang[1,2], Terence Kin-Wah Lee[9], Stephanie Ma[10], Mu-Sheng Zeng[1], Jing-Ping Yun[1,2,*]

[1]*Sun Yat-sen University Cancer Center, State Key Laboratory of Oncology in Southern China, Collaborative Innovation Center for Cancer Medicine, Guangzhou, Guangdong, 510060, China;* [2]*Department of Pathology, Sun Yat-sen University Cancer Center, Guangzhou, Guangdong, 510060, China;* [3]*MOE Key Laboratory of Tumor Molecular Biology and Key Laboratory of Functional Protein Research of Guangdong Higher Education Institutes, Institute of Life and Health Engineering, College of Life Science and Technology, Jinan University, Guangzhou, 510632, China;* [4]*Department of Anatomical Pathology, Singapore General Hospital, Singapore, 169856, Singapore;* [5]*Institute of Molecular Cell Biology (IMCB), Agency of Science, Technology and Research (A*STAR), Singapore, 169856, Singapore;* [6]*Singapore Immunology Network, Agency of Science (SIgN), Technology and Research (A*STAR), Singapore, 169856, Singapore;* [7]*Department of Molecular Diagnosis, Sun Yat-sen University Cancer Center, Guangzhou, Guangdong 510060, China;* [8]*Center for Infection and Immunity Study, School of Medicine, Sun Yat-sen University, Guangzhou, China;* [9]*Department of Applied Biology and Chemical Technology, The Hong Kong Polytechnic University, Hong Kong;* [10]*School of Biomedical Sciences, Li Ka Shing Faculty of Medicine, The University of Hong Kong, Hong Kong*

Background & Aims: Little is known about Epstein-Barr virus (EBV)-associated intrahepatic cholangiocarcinoma (EBVaICC) because of its rarity. We aimed to comprehensively investigate the clinicopathology, tumor immune microenvironment (TIME) and genomic landscape of this entity in southern China.

Methods: We evaluated 303 intrahepatic cholangiocarcinomas (ICCs) using *in situ* hybridization for EBV. We compared clinicopathological parameters between EBVaICC and nonEBVaICC, and we analyzed EBV infection status, tumor-infiltrating lymphocytes (TILs) and genomic features of EBVaICC by immunohistochemistry, double staining, nested PCR, multiplex immunofluorescence staining, fluorescence *in situ* hybridization and whole-exome sequencing.

Results: EBVaICC accounted for 6.6% of ICCs and was associated with EBV latency type I infection and clonal EBV isolates. Patients with EBVaICC were more often female and younger, with solitary tumors, higher HBV infection rates and less frequent cirrhosis; the lymphoepithelioma-like (LEL) subtype was more common in EBVaICC. EBVaICC was associated with a significantly larger TIME component than nonEBVaICC. The LEL subtype of EBVaICC – associated with a significantly increased density and proportion of CD20+ B cells and CD8+ T cells – was associated with significantly higher 2-year survival rates than conventional EBVaICC and nonEBVaICC. Both PD-1 and PD-L1 in TILs, and PD-L1 in tumor cells, were overexpressed in EBVaICC. High PD-L1 expression in tumor cells and high CD8+ TIL densities were significantly more common in EBVaICC than in nonEBVaICC. Seven genes (*MUC4*, *DNAH1*, *GLI2*, *LIPE*, *MYH7*, *RP11-766F14.2* and *WDR36*) were mutated in at least 3 patients. EBVaICC had a different mutational pattern to liver fluke-associated cholangiocarcinoma and HBV-associated ICC.

Conclusions: EBVaICC, as a subset of ICC, has unique etiological, clinicopathological and genetic characteristics, with a significantly larger TIME component. Paradoxically, patients with EBVaICC could be candidates for immune checkpoint therapy.

Lay summary: Epstein-Barr virus (EBV) is associated with a subtype of intrahepatic cholangiocarcinoma, with unique clinicopathological and genetic characteristics. The tumor immune microenvironment is also different in this tumor subtype and patients with EBV-associated intrahepatic cholangiocarcinoma may respond well to immune checkpoint inhibitors.

Introduction

Intrahepatic cholangiocarcinoma (ICC) is the second most common malignancy of the liver, with a much higher incidence in parts of the Eastern world compared to the West.[1] The incidence of ICC has been rising globally over recent decades,[2] and the etiology and pathogenesis are still not fully understood. ICC is associated with low survival rates because of its biological aggressiveness and poor resectability, but also because current therapeutic options remain limited.[3] Currently, approximately 50% of cases are still diagnosed without any identifiable risk factors.[4,5]

Epstein-Barr virus (EBV) has been linked to several carcinomas of the aerodigestive tract, especially undifferentiated

Keywords: Epstein-Barr virus; Intrahepatic cholangiocarcinoma; Clinicopathology; Tumor immune microenvironment; Genomic landscape.
Received 13 May 2020; received in revised form 7 October 2020; accepted 30 October 2020; available online 17 November 2020

* Corresponding author. Address: Department of Pathology, Sun Yat-sen University Cancer Center, Guangzhou, Guangdong, 510060, China. Tel.: +86-2087343693, fax: +86-2087343702.
E-mail address: yunjp@sysucc.org.cn (J.-P. Yun).
† Yu-Hua Huang, Chris Zhi-yi Zhang and Qun-Sheng Huang shares co-first authorship.

https://doi.org/10.1016/j.jhep.2020.10.037

nasopharyngeal carcinoma (NPC)[6] and EBV-associated gastric carcinoma (EBVaGC),[7] but the relationship between EBV infection and ICC pathogenesis has not been well characterized. The current level of evidence on EBV-associated ICC (EBVaICC) is solely based on case reports and small series.[8–11] Of note, the vast majority of previously reported EBVaICC cases arose in Asia in patients of Chinese descent,[8–11] which showed a remarkable ethnic and geographical distribution. To date, little is known about EBVaICC. Thus, a systematic and deeper understanding of this rare entity is required to elucidate its pathogenesis and identify potential therapeutic strategies.

Herein, we identified the EBV infection status of a large cohort of patients with ICC in southern China, which has the highest incidence of EBV-associated NPC.[12] In addition, we systematically analyzed the clinicopathological features and tumor immune environment (TIME) of EBVaICC. We also report on a patient with EBVaICC who survived for 84 months, having exhibited a marked response to combined therapy with immune checkpoint blockade. Furthermore, we also study, for the first time, the genomic landscape of EBVaICC and ICC-associated EBV.

Materials and methods

Patients, samples and clinicopathological data

A retrospective consecutive cohort of 303 patients with ICC who primarily underwent their first surgical resection at Sun Yat-sen University Cancer Center, Guangzhou, China, between April 2008 and May 2017, were included in this study. The well-known risk factors of ICC[4,5] identified in the present cohort are listed in Table S1. The median follow-up period of surviving patients was 50 months. All patients provided written informed consent for the collection and publication of their medical information during the first visit to the hospital. The study was approved by the Sun Yat-sen University Cancer Center clinical research ethics committee. The authenticity of this article has been validated by uploading the key raw data onto the Research Data Deposit public platform (www.researchdata.org.cn) with approval number RDDB2020000851. All specimens were formalin-fixed and paraffin-embedded, processed routinely and H&E stained. The histological slides were retrieved and reviewed; the diagnosis was confirmed by 2 experienced digestive pathologists. The lymphoepithelioma-like (LEL) subtype of ICC was defined as follows: i) more lymphocytes than tumor cells, ii) no desmoplasia throughout the tumor, and iii) tumor cells consistent with the immunophenotype of ICC.

Tissue microarray construction and EBV-encoded RNA *in situ* hybridization

EBV Probe *in situ* hybridization (ISH) Kit (ISH-6021, Zhongshan Golden Bridge Biotechnology) was used to detect EBV-encoded RNA (EBER) in tissue microarray (TMA) slides according to the manufacturer's protocol.

Double staining

To demonstrate the presence of EBV in tumor cells, CK7 immunohistochemistry plus EBER *in situ hybridization* dual-staining technique was performed. In addition, double immunohistochemical staining for CK7 and EBNA1 was utilized.

Nested PCR and real-time quantitative PCR

EBV clonality was evaluated in all EBVaICC samples using nested PCR amplification of LMP-1 33 base pair repeats as previously reported.[13] Real-time quantitative PCR was applied toward the BamHI-W region for EBV DNA detection in 15 serum samples from patients with EBVaICC.

Immunohistochemical staining and analysis

IHC was performed to analyze the expression of latent EBV proteins (Epstein-Barr nuclear antigen 1 and 2 [EBNA1 and EBNA2], and latent membrane protein 1 [LMP1]) in all EBVaICC cases using a BenchMark ULTRA automatic immunostaining device according to the manufacturer's instructions. In addition, IHC was applied to evaluate the immunophenotype of tumor cells and tumor-infiltrating lymphocytes (TILs) in all 303 ICCs. After IHC staining for CD20, CD3, CD68, CD8, FoxP3, cytotoxic T-lymphocyte-associated protein 4 (CTLA-4), HLA-DR and CD163, TMA slides were scanned by a digital pathology scanner (Aperio AT2, Leica). The average density (cells/mm^2) of each lymphocyte subset was quantitatively scored with the HALO 2.3 Digital Pathology system (Indica Labs) in a whole TMA core. Programmed cell death ligand 1 (PD-L1) expression in tumor cells and in TILs, and programmed cell death 1 (PD-1) expression in TILs, were scored using an immunoreactivity scoring system (IRS) based on the percentage and staining intensity of stained cells (Table S2). CD8+ T cell densities were divided into 2 groups (high *vs.* low) according to a median split. Based on the expression status of PD-L1 in tumor cells and tumor-infiltrating CD8+ T cell densities, ICCs were categorized into 4 tumor microenvironment types (TMITs): Type I (PD-L1+/CD8^{-High}), Type II (PD-L1-/CD8^{-low}), Type III (PD-L1+/CD8^{-low}) and Type IV (PD-L1-/CD8^{-High}).[14]

Multiplex immunofluorescence staining and evaluation

Multiplex immunofluorescence staining was carried out with Opal 7-Color Manual IHC Kits (Panovue Biotechnology) according to the manufacturer's protocol. Two panels, including CD20, CD3 and CD8, as well as CK, PD-L1 and CD8, were visualized with Vectra 2 System and Nuance and InForm image analysis software (PerkinElmer).

Fluorescence *in situ* hybridization

To detect *FGFR2* gene translocation and *PD-L1* gene amplification, *FGFR2* (10q26) split dual-color probe and *PD-L1*/CEN9q dual-color probe (LBP Medicine Science and Technology Co., Ltd) were utilized for fluorescence *in situ* hybridization (FISH) in all EBVaICC cases, respectively.

Whole-exome sequencing

The 20-fresh tumor/control paired tissue samples isolated from 10 EBVaICC patients were sequenced using commercial DNA sequencing services (Guangzhou Gene Denovo Biotechnology). The raw sequence data reported in this paper have been deposited in the Genome Sequence Archive of the BIG Data Center at the Beijing Institute of Genomics, Chinese Academy of Science, under accession number HRA000346 (http://bigd.big.ac.cn/gsa-human). Code is available from corresponding author on reasonable request. The 5 new hotspots in ICC-derived EBV identified by whole-exome sequencing (WES) (Table S3) were further validated by Sanger sequencing.

Statistical analysis

The overall survival (OS) time was defined as the period of time in months from operation to death. Relapse-free survival (RFS) time was assessed from the day of tumor

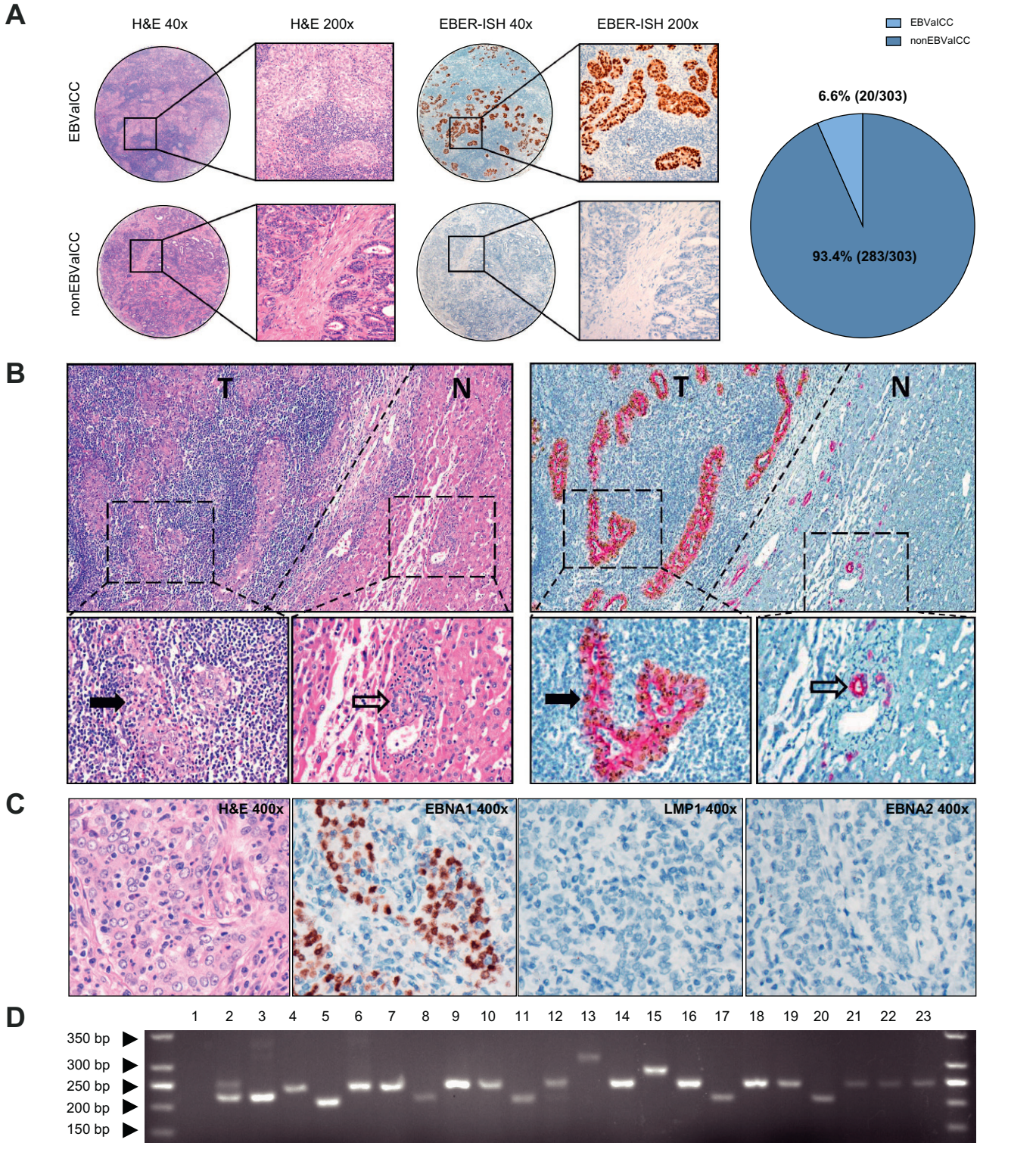

Fig. 1. Prevalence and EBV infection status of EBVaICC. (A) EBER-ISH in ICC on TMA, showing representative cases of EBVaICC and nonEBVaICC; EBVaICC accounted for 6.6% (20/303) of ICC. (B) Double staining for EBER (brown) and CK7 (red) showing that EBV was only present in the nuclei of tumor cells (solid arrow) but not observed in adjacent benign bile duct epithelia (hollow arrow). (C) EBVaICC expressed EBNA1 but not EBNA2 and LMP1, which suggested that EBV harbored in EBVaICC belonged to latency type I infection. (D) Nested PCR amplification of the 33 base pair variable repeat region. Lane 1, blank control; Lane 2, polyclonal control (infectious mononucleosis sample); Lane 3, monoclonal control (Raji cell); Lanes 4-23, EBVaICC samples, a single band indicated clonal EBV isolates in each EBVaICC case. EBNA1, Epstein-Barr nuclear antigen 1; EBNA2, Epstein-Barr nuclear antigen 2; EBER, Epstein-Barr virus-encoded RNA; EBV, Epstein-Barr virus; EBVaICC, EBV-associated intrahepatic cholangiocarcinoma; ICC, intrahepatic cholangiocarcinoma; ISH, *in situ* hybridization; LMP1, latent membrane protein 1; TMA, tissue microarray.

resection to disease recurrence. The high and low TIL density/proportion was defined as above and below a cut-off determined using receiver operating characteristic (ROC) curves and the area under the ROC curve (AUC). Statistical analyses were performed using SPSS 23.0 for Windows (IBM). A comparison between groups was conducted using the Wilcoxon rank-sum, chi-square or Fisher's exact test for categorical variables and the t-test for discrete variables. Survival analysis was performed using the Kaplan-Meier and Life Table method. The value of $p<0.05$ was considered to be statistically significant.

The technique used for each EBVaICC sample is shown in Table S4. For further details regarding the materials used, please refer to the CTAT table and supplementary information.

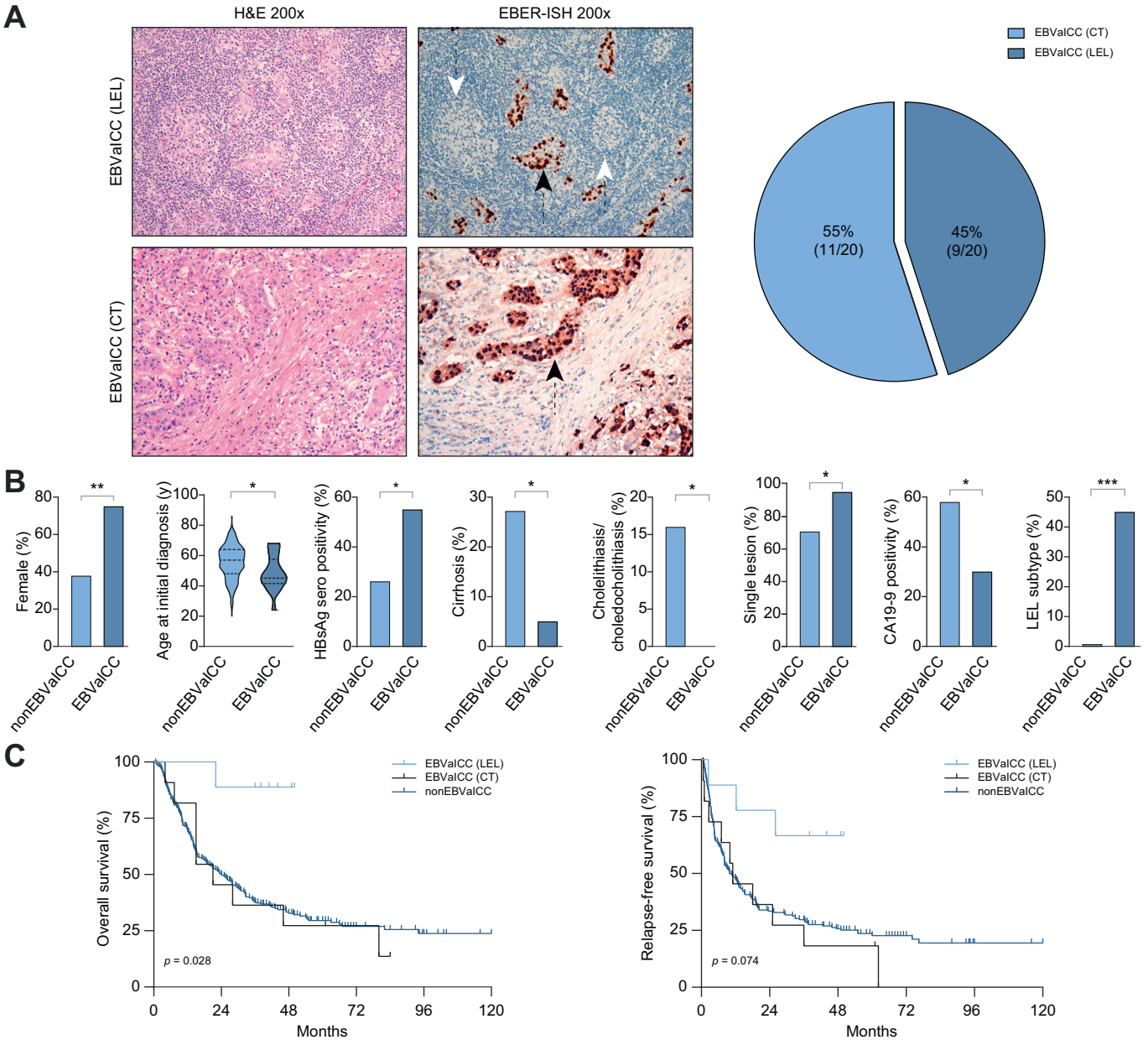

Fig. 2. Differences in clinicopathological and prognostic characteristics between EBVaICC and nonEBVaICC. (A) Representative morphology of the LEL subtype and CT of ICC were identified among EBVaICC; LEL subtype and CT were identified in 45% and 55% of EBVaICC, respectively. (B) EBVaICC tended to occur predominantly in females, younger patients with solitary tumors, lower cirrhotic backgrounds, higher HBsAg seropositive rates, lower cholelithiasis/choledocholithiasis rate, lower serum CA19-9 levels and increased LEL subtype proportion (all p values <0.05, based on chi-square & Fisher's exact test). (C) Patients with EBVaICC (LEL subtype) had a significantly longer OS than EBVaICC (CT) and nonEBVaICC ($p = 0.028$), but not significant for RFS ($p = 0.074$), based on Kaplan-Meier survival analyses. CT, conventional type; EBV, Epstein-Barr virus; EBVaICC, EBV-associated intrahepatic cholangiocarcinoma; ICC, intrahepatic cholangiocarcinoma; LEL subtype, lymphoepithelioma-like subtype; OS, overall survival; RFS, relapse-free survival.

Results

Prevalence and EBV infection status of ICC

EBERs were detected in 6.6% (20/303) of primary ICCs (Fig. 1A) and were not observed in any detected perihilar cholangiocarcinoma (pCCA), distal cholangiocarcinoma (dCCA), combined mixed hepatocellular and cholangiocarcinoma (cHCC-CCA), or hepatocellular carcinoma (HCC) (Fig. S1). Double staining revealed that EBV was only detected in the EBVaICC tumor cells but was not present in adjacent non-neoplastic bile duct epithelium (Fig. 1B and Fig. S2). All EBVaICCs were positive for EBNA1 but were negative for LMP1 and EBNA2, which suggested that EBV belonged to the latency type I infection (Fig. 1C). Nested PCR amplification of LMP-1 33 base pair repeats indicated clonal EBV isolates in all 20 EBVaICCs (Fig. 1D).

Clinical characteristics of EBVaICC

The ages of patients with EBVaICC ranged from 24 to 68 years, with a median age of 46.5 years. There was a predominance of females, with the male-to-female ratio of 1:3. All patients were Chinese. Ten patients (50%) showed HBsAg seropositivity, and only 1 patient (5%) had histologically confirmed cirrhosis. Nineteen patients (95%) harbored a solitary tumor. According to AJCC TNM staging (8th Edition), 14 patients (70%) were classified as stage I/II, and 6 patients (30%) were classified as stage III/IV. Serum EBV DNA>1,000 copy/ml was present in 2 out of 15 (13.3%) available cases (Table S5).

Morphology and immunophenotype of EBVaICC

Pathological data for EBVaICC, including histology, immunohistochemistry and *in situ* hybridization, are summarized in Tables S6-7. Histologically, the lymphoepithelioma-like subtype and conventional type of ICC were identified in 45% (9/20) and 55% (11/20) of EBVaICCs, respectively (Fig. 2A). Secondary lymphoid follicles were found within the tumor in all cases of the LEL subtype of EBVaICC but not in any of the conventional type of EBVaICC (Fig. 2A). All EBVaICCs exhibited variable expression of biliary-type cytokeratins (CK7 and CK19) (Table S7) and showed immunopositivity for missense repair proteins of microsatellite instability (MLH1, PMS2, MSH2 and MSH6) (Fig. S3 and Table S7).

Clinicopathological characteristics between EBVaICC and nonEBVaICC

EBV infection was not significantly related to any well-known risk factors of ICC, except for HBV (Table S1). Compared to patients with nonEBVaICC, EBVaICC tended to occur predominantly in females (75.0% *vs.* 37.8%), younger patients (median age 46.5 *vs.* 57.0 years-old) with a higher HBsAg seropositive rate (50.0% *vs.* 26.1%), lower cirrhotic background (5.0% *vs.* 27.2%), lower cholelithiasis/choledocholithiasis rate (0% *vs.* 16.8%), solitary tumors (95.0% *vs.* 70.7%), and lower serum CA19-9 positive rate (30.0% *vs.* 58.0%) (all p values <0.05). Histologically, the LEL subtype of ICC was significantly more commonly found in EBVaICC than in nonEBVaICC (45% *vs.* 0.7%, p <0.001), indicating the LEL subtype had a close relationship with EBV infection (Fig. 2A-2B). Differences in clinicopathological features between EBVaICC and other infection-related ICCs in this cohort, including liver fluke-associated ICC (LFaICC) and HBV-associated ICC (HBVaICC), are shown in Table S9 and Fig. S4.

Prognostic significance of EBVaICC

Although EBV infection was not significantly related to OS and RFS in ICC (Fig. S5), EBVaICC (LEL subtype) was associated with a significantly better 2-year OS rate (89%) than conventional EBVaICC (36%) and nonEBVaICC (38%) (p = 0.028). The 2-year RFS rate for EBVaICC (LEL subtype) was 67%, which was higher than, but not significantly different from those for conventional EBVaICC (27%) and nonEBVaICC (30%) (p = 0.074) (Fig. 2C). Of note, EBVaICC was associated with significantly better 2-year OS and RFS rates than HBVaICC and LFaICC (Fig. S4).

Tumor-infiltrating lymphocytes in EBVaICC

TILs in EBVaICC were predominately CD3+ T cells (84.4% ± 3.6%), CD20+ B cells (9.4% ± 2.8%) and CD68+ tumor-associated macrophages (TAMs) (6.1% ± 1.1%). Among the T cell population, CD8+ T cells accounted for 71.4% ± 2.9%, while FoxP3+ T cells and CTLA-4+ T cells accounted for 15.0% ± 2.0% and 13.6% ± 1.9%, respectively. HLA-DR+ M1 TAMs (77.6% ± 2.9%) were predominant compared to CD163+ M2 TAMs (22.4% ± 2.9%) in EBVaICC. The proportion of CD20+ B cell as well as CD8+ T cell populations were significantly increased in EBVaICC compared to non-EBVaICC, while no difference in the M1/M2 TAM ratio was identified (Fig. S6).

The densities of tumor-infiltrating immune cells, including CD20+ B cells, CD3+ T cells, CD68+ TAMs, CD8+ T cells, FoxP3+ T cells, CTLA-4+ T cells, HLA-DR+ M1 TAMs and CD163+ M2 TAMs were significantly increased in EBVaICC compared with non-EBVaICC (all p values <0.01) (Fig. 3A-B). Of note, EBVaICC had a significantly larger TIME component than HBVaICC and LFaICC; no difference was observed between HBVaICC and LFaICC (Fig. S7).

As shown in (Fig. 4A-B), the EBVaICC LEL subtype had significantly higher densities of CD20+ B, CD3+ T and CD8+ T cells compared with conventional EBVaICC and nonEBVaICC (p <0.05 for all comparisons). Of note, increased densities of CD20+ B and CD8+ T cells were significantly related to longer OS and RFS in ICC, respectively (p <0.05 for all comparisons) (Fig. 4C).

Association between EBV positivity and expression of PD-1 and PD-L1

Both PD-1 and PD-L1 in TILs, and PD-L1 in tumor cells, were overexpressed in EBVaICC. A total of 95.0% (19/20) of EBVaICCs were positive for PD-L1 in tumor cells (IRS score≥3) but only 22.3% (63/283) of nonEBVaICCs were (p <0.0001); 100% (20/20) of EBVaICCs were positive for PD-L1 in TILs (IRS score≥1) but only 56.5% (160/283) of nonEBVaICCs were (p <0.0001). A total of 95.0% (19/20) of EBVaICCs were positive for PD-1 in TILs (IRS score≥1) but only 64.0% (181/283) of nonEBVaICCs were (p = 0.005) (Fig. 5A-B). Interestingly, *PD-L1* gene amplification was not observed in 95% (19/20) of EBVaICCs by FISH analysis (Fig. 5A, inset figure). The IHC expression patterns of PD-L1 and PD-1 in all 303 ICC cases are shown in Fig. 5C.

Association between EBV positivity and TMIT

We classified each ICC sample into a TMIT (type I, II, III and IV) according to immunohistochemical results as follows: Type I, 53 samples (17.5%); Type II, 123 (40.6%); Type III, 29 (9.6%); and Type IV, 98 (32.3%) (Fig. 6A). TMIT was significantly related to OS in ICC (p = 0.014) but not significant for RFS (p = 0.059) (Fig. 6B). The TMIT I subgroup had the best survival benefit, and the TMIT III subgroup had the worst survival benefit.

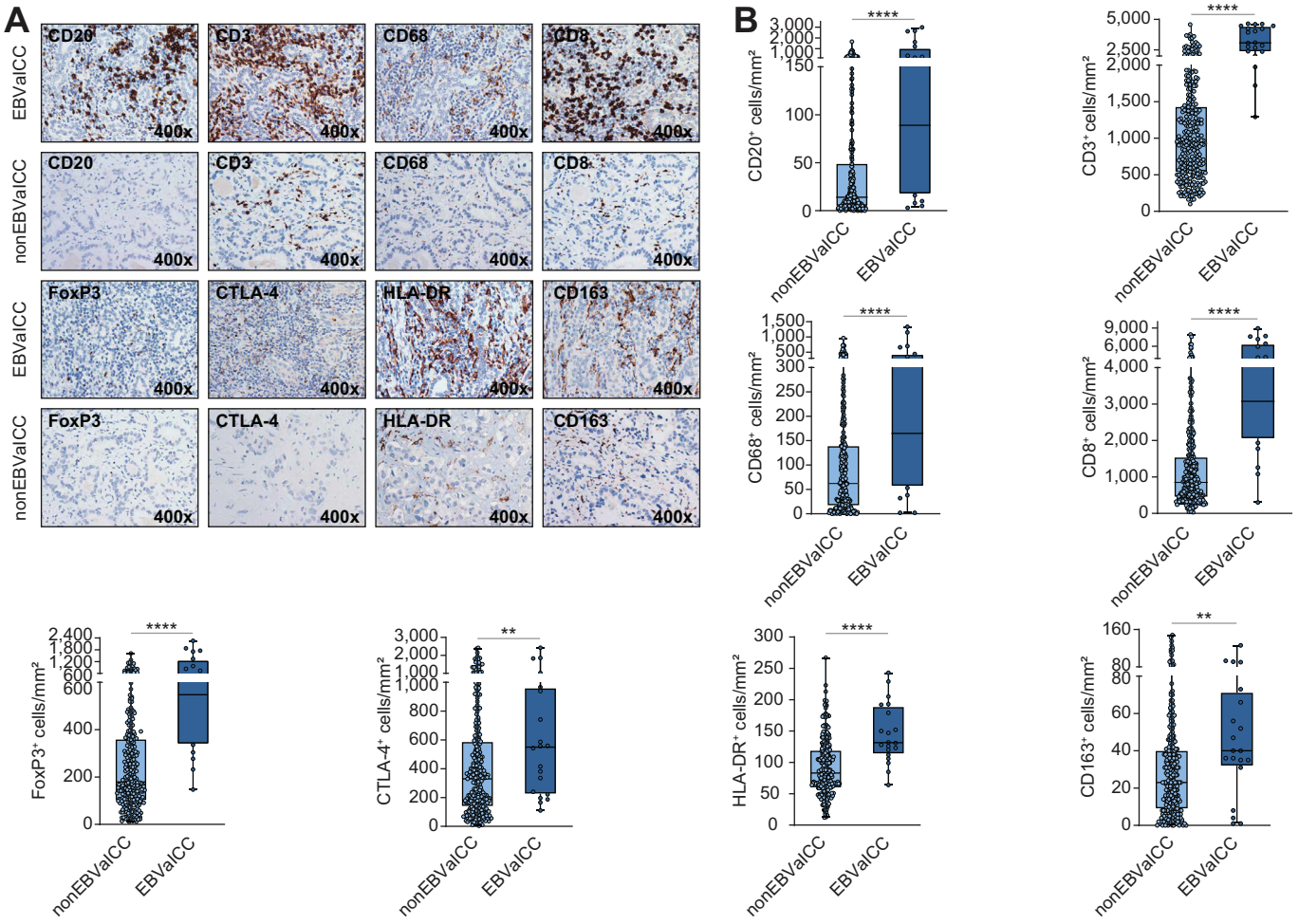

Fig. 3. Densities of TILs were significantly increased in EBVaICC compared with nonEBVaICC. (A) Representative IHC images of TILs in EBVaICC and non-EBVaICC. (B) The density of tumor-infiltrating CD20+ B lymphocytes, CD3+ T lymphocytes and CD68+ TAMs were significantly increased in EBVaICC compared with nonEBVaICC as well as CD8+, PoxP3+ and CTLA4+ T cell populations and HLA-DR+M1 TAMs and CD163+ M2 TAMs (all p values <0.01, based on t-test). EBV, Epstein-Barr virus; EBVaICC, EBV-associated intrahepatic cholangiocarcinoma; IHC, immunohistochemical; TAMs, tumor-associated macrophages; TILs, tumor-infiltrating lymphocytes.

Clinicopathological relationships between TMIT and CD8 or PD-L1 expression are shown in Table S10. Of note, EBVaICC was significantly associated with TMIT I because 90% (18/20) of EBVaICCs belonged to TMIT I, while the value was only 12.4% (35/283) for nonEBVaICCs (p <0.0001) (Fig. 6C). The patient from Case #4 exhibited a marked response to the combined therapy, including immune checkpoint inhibitor therapy, with a long survival time of 84 months; patient details are provided in Table S5-7 and Fig. S8. Interestingly, EBVaICC had a significantly different TMIT (in addition to having significantly elevated TILs and harboring high PD-L1 expression) than HBVaICC and LFaICC (Table S11-12).

Somatic aberrations of EBVaICC

We analyzed the WES data of 10 EBVaICCs with a mean coverage of 100x and identified 3,353 somatic synonymous and non-synonymous mutations (including single-nucleotide mutations and small insertions and deletions, or InDels). The somatic mutations included 1,346 non-silent and 2,007 silent mutations, which revealed a high mutation rate (median: 4.4 mutations per megabase). We discovered that 7 genes were affected by non-silent mutations in at least 3 patients, including *MUC4*, *DNAH1*, *GLI2*, *LIPE, MYH7, RP11-766F14.2* and *WDR36*. The predominant somatic mutation type was C: G>T: A transitions and C: G>A: T transitions. Then, 3 independent and stable mutational signatures were identified (Fig. S9). In addition, 22 potential driver genes in EBVaICC were predicted by the MuSigCV software (Fig. 7). Significantly mutated genes in EBVaICC compared to those reported in ICC[15] are shown in Fig. S10. Of note, EBVaICC displayed a different mutational pattern from other EBV-associated carcinomas including EBVaGC,[16] NPC[17] and pulmonary lymphoepithelioma-like carcinoma[18] (Fig. S11), and other infection-related CCA, including HBVaICC[15] and LFaCCA[19,20] (Fig. S12).

Somatic copy number alterations of EBVaICC

Frequent alterations included copy number losses in 7q34 (q-value = 2.3168e-07, 30%) and 14q11.2 (q-value <1e-07, 50%). No frequent arm-level alterations for copy number gains were noted. When mutations of druggable genomes in Maftools with

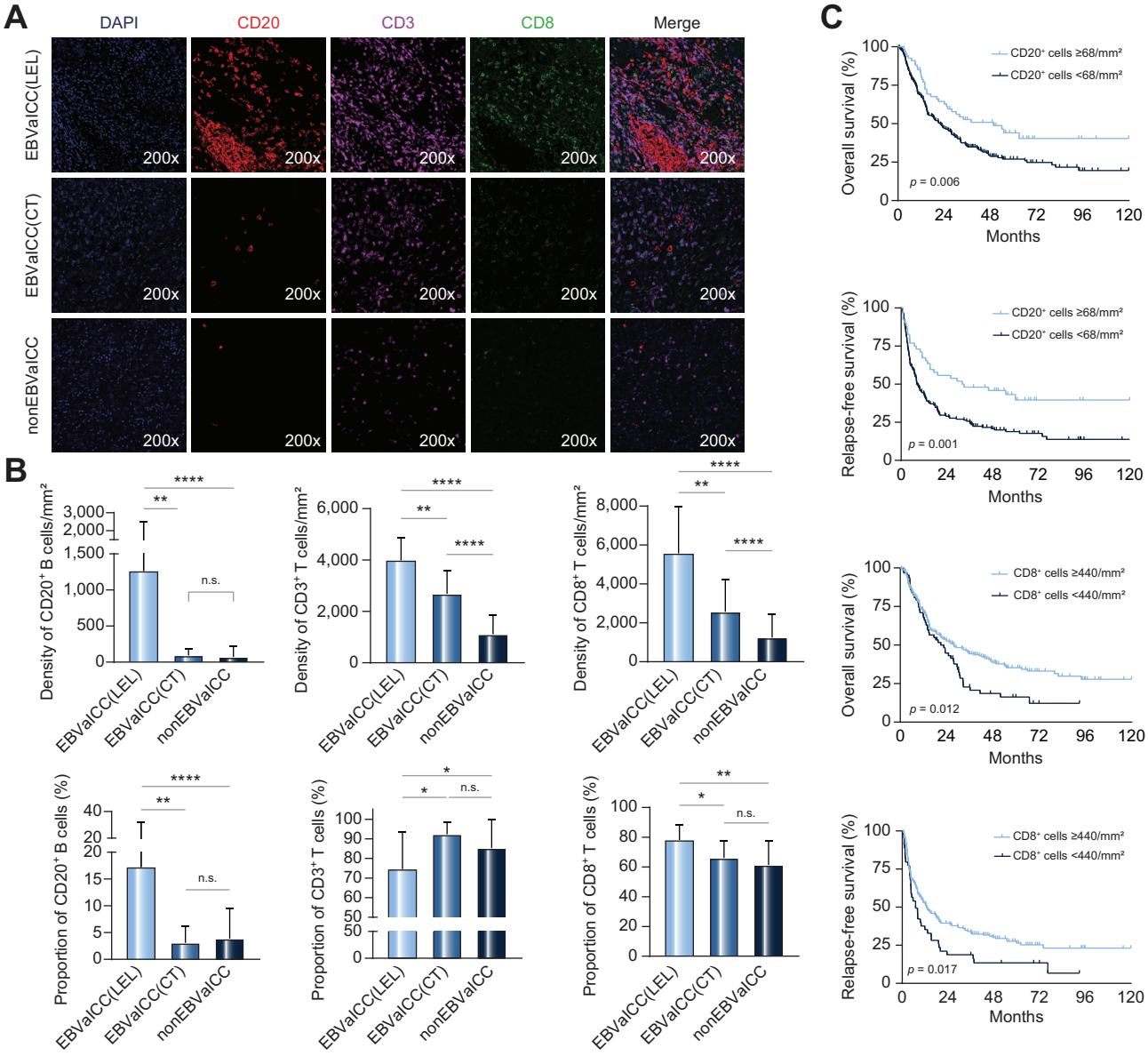

Fig. 4. Proportions and densities of tumor-infiltrating CD20+ B cells and CD8+ T cells were significantly increased in the LEL subtype of EBVaICC. (A) Representative multiple immunofluorescence images of CD20, CD3 and CD8 in EBVaICC (LEL subtype), EBVaICC (CT) and nonEBVaICC. (B) The proportions and densities of tumor-infiltrating CD20+ B cells and CD8+ T cells were significantly increased in the LEL subtype of EBVaICC, (all *p* values <0.05, based on t-test). (C) The densities of CD20+ cells and CD8+ T cells were significantly related to OS and RFS in ICC, respectively, based on Kaplan-Meier survival analyses. CT, conventional type; EBV, Epstein-Barr virus; EBVaICC, EBV-associated intrahepatic cholangiocarcinoma; ICC, intrahepatic cholangiocarcinoma; LEL subtype, lymphoepithelioma-like subtype; OS, overall survival; RFS, relapse-free survival.

information compiled from the Drug Gene Interaction database were analyzed, deletions of *PRSS1*, which was regarded as disease-causative in pancreatitis,[21] were identified in 3 cases (30%) (Fig. S13). The amplification of *CD274* was not identified among these 10 cases. Amplification of *CD274* was associated with elevated PD-L1 expression in EBVaGC.[22] Altered pathways enriched in EBVaICC are shown in Fig. S14.

Somatic structural variation

FGFR2 gene fusions were not detected in 10 EBVaICC cases in WES data by novoBreak algorithm, which were validated by FISH analysis using a split dual-color probe.

Single-nucleotide variant of the EBV genome in EBVaICC

The top 40 frequent nonsynonymous mutations identified in ICC-derived EBV are shown in Fig. 8, which were determined by aligning the viral reads against the EBV reference genome (NC_007605.1). All cases harbored new hotspots of *BKRF4* (H171N), *BcRF1* (T33A), *BKRF4* (G169V), *BOLF1* (D1154E) and *BPLF1* (S405G). All of these hotspots were successfully validated in tumor tissues by Sanger sequencing, except for BPLF1 (S405G), the mutation validation of which failed due to high GC DNA templates (Fig. S15). Mutations were frequently observed in the *BRLF1*, *BOLF1* and *BRRF2* regions. Of note, variants in *BOLF1* and *BRRF2* are significantly enriched in ICC, other than those at

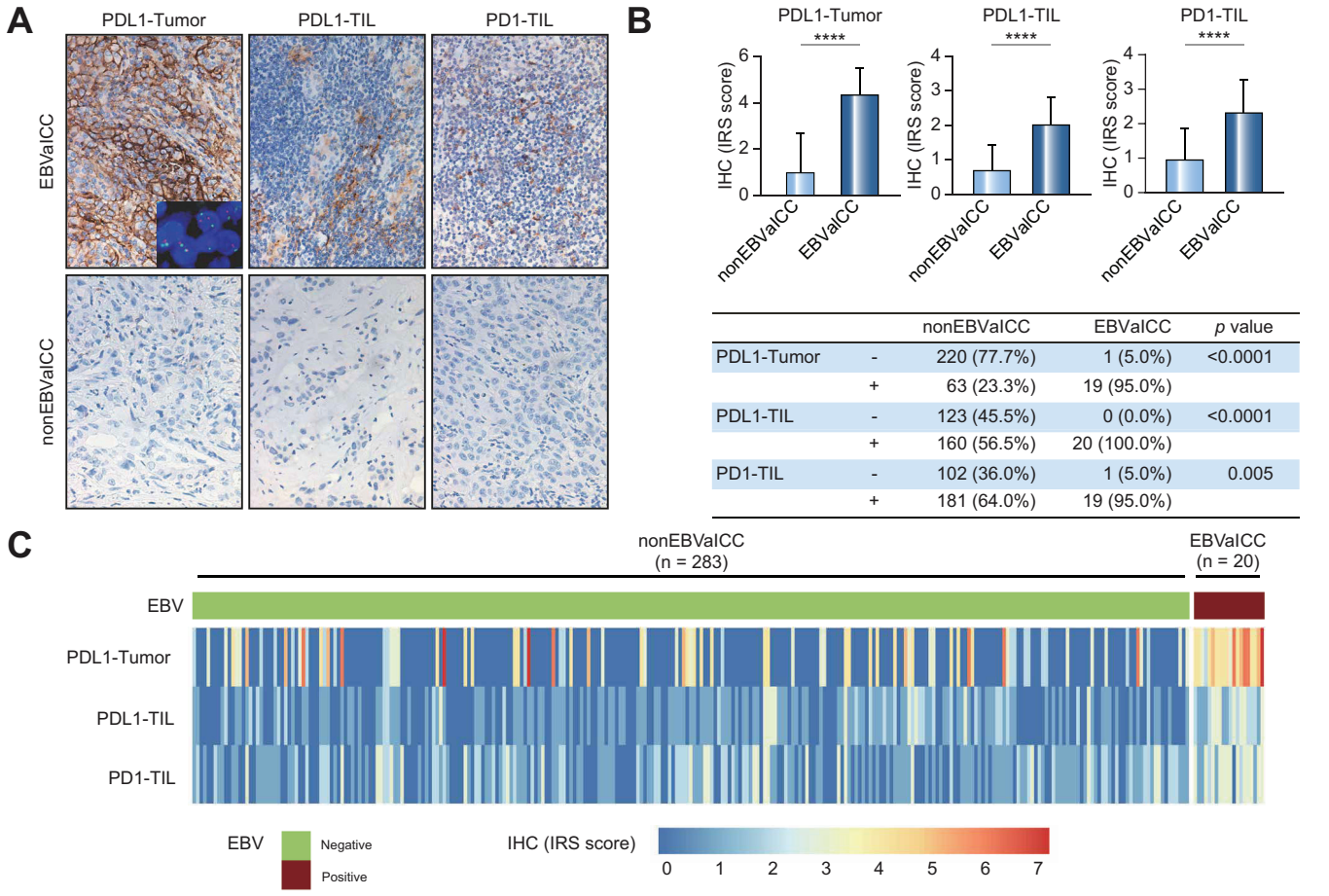

		nonEBVaICC	EBVaICC	*p* value
PDL1-Tumor	-	220 (77.7%)	1 (5.0%)	<0.0001
	+	63 (23.3%)	19 (95.0%)	
PDL1-TIL	-	123 (45.5%)	0 (0.0%)	<0.0001
	+	160 (56.5%)	20 (100.0%)	
PD1-TIL	-	102 (36.0%)	1 (5.0%)	0.005
	+	181 (64.0%)	19 (95.0%)	

Fig. 5. EBVaICC harbored high PD-L1/PD-1 expression. (A) Tumor cells were positive for PD-L1, and TILs were positive for both PD-L1 and PD-1 in a representative case of EBVaICC (IHC) without *PD-L1* gene amplification (inset figure, FISH), while either PD-L1 or PD-1 was negative in nonEBVaICC (IHC). (B) Differences in IHC expression of PD-1 and PD-L1 between EBVaICC and nonEBVaICC, based on chi-square & Fisher's exact test. (C) PD-L1 and PD-1 expression in EBVaICC and nonEBVaICC. EBV, Epstein-Barr virus; EBVaICC, EBV-associated intrahepatic cholangiocarcinoma; FISH, fluorescence *in situ* hybridization; IHC, immunohistochemical; TILs, tumor-infiltrating lymphocytes.

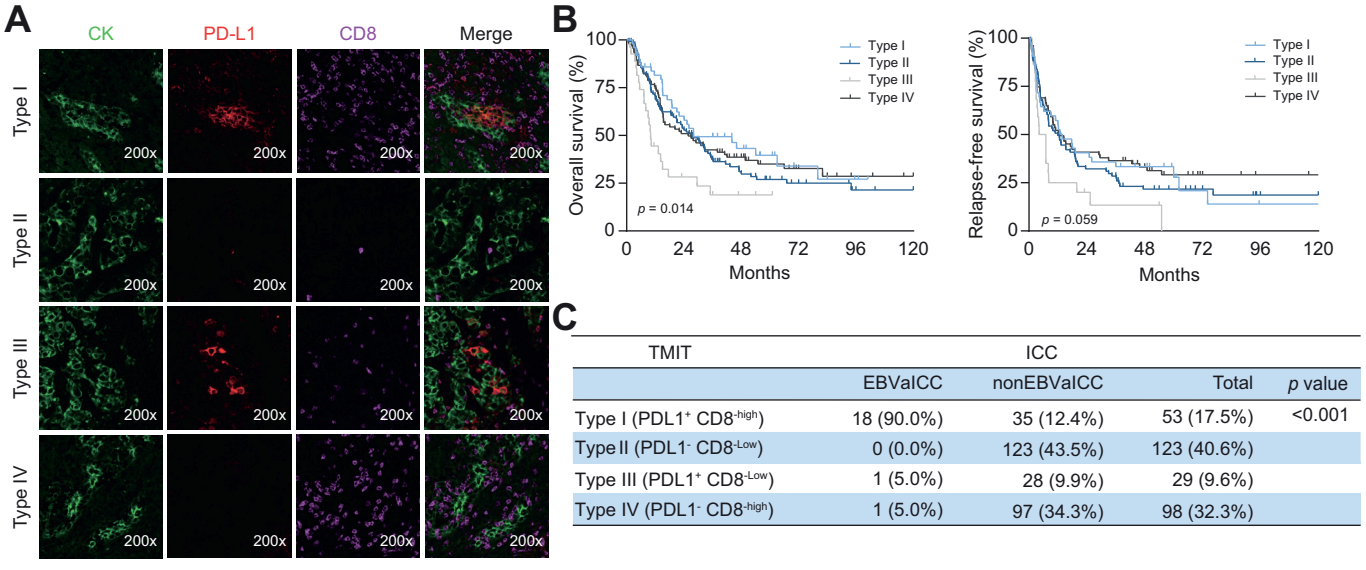

C

TMIT	ICC			
	EBVaICC	nonEBVaICC	Total	*p* value
Type I (PDL1^{+} CD8^{-High})	18 (90.0%)	35 (12.4%)	53 (17.5%)	<0.001
Type II (PDL1^{-} CD8^{-Low})	0 (0.0%)	123 (43.5%)	123 (40.6%)	
Type III (PDL1^{+} CD8^{-Low})	1 (5.0%)	28 (9.9%)	29 (9.6%)	
Type IV (PDL1^{-} CD8^{-High})	1 (5.0%)	97 (34.3%)	98 (32.3%)	

Fig. 6. TMIT was related to the EBV infection in ICC. (A) Four TMITs in ICC (multiplex immunofluorescence staining). (B) OS ($p = 0.014$) and RFS ($p = 0.059$) proportion of patients with ICC stratified by TMITs, based on Kaplan-Meier survival analyses. (C) Relationship between EBV infection and TMIT in ICC. TMIT I (PD-L1 Tumor+ CD8^{-High}) was significantly more common in EBVaICC than in nonEBVaICC (p <0.001), based on Fisher's exact test). EBV, Epstein-Barr virus; EBVaICC, EBV-associated intrahepatic cholangiocarcinoma; ICC, intrahepatic cholangiocarcinoma; OS, overall survival; RFS, relapse-free survival; TMIT, tumor environment immune type.

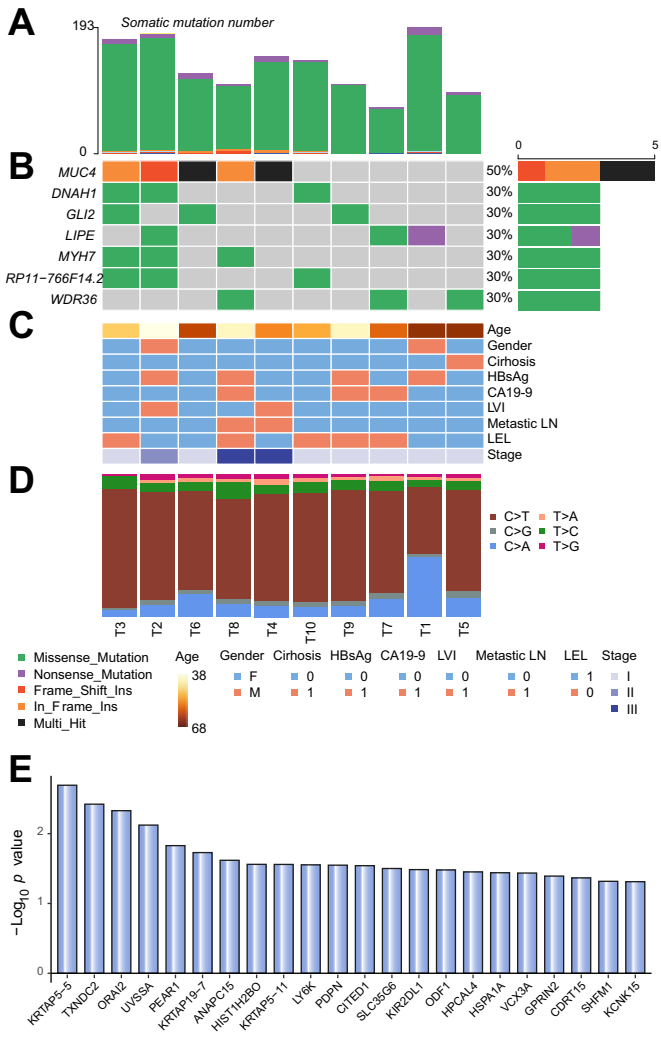

Fig. 7. Somatic mutations in EBVaICC. (A) Number of somatic mutation genes for each EBVaICC sample. (B) Frequently mutated genes (identified in at least 3 samples) in EBVaICC. (C) Clinicopathological features are listed according to the samples. (D) Predominant somatic mutation type for each EBVaICC sample. (E) Twenty-two potential driven genes identified by the MuSigCV algorithm are shown, with the x-axis showing mutation types and the y-axis showing the estimated mutations. EBVaICC, EBV-associated intrahepatic cholangiocarcinoma.

EBNAs, *LMP1*, *LMP2* and *BDLF2/3*, which were consistently reported in EBV derived from other cancers.[23,24]

Discussion

To date, the EBV infection status of ICC in southern China, with the highest incidence of EBV-associated NPC,[12] still remains unknown. Our results revealed for the first time that the overall prevalence of EBVaICC was 6.6%, which was similar to that of EBVaGC (5.1%) in this area.[7] In addition, all EBVaICCs were positive for EBNA1, without immunostaining for LMP1 and EBNA2, which indicated that EBV harbored in ICC was a latency type I infection. Furthermore, EBV was detected in EBVaICC tumor cells with clonal isolates but was not present in adjacent non-neoplastic bile duct epithelium. Such observations imply that EBV infection may have occurred before the expansion of the malignant cell clone or arose from a single infected progenitor cell.

In this study, EBV infection was only detected in ICC but not observed in the limited cases of pCCA, dCCA and cHCC-CCA, which indicated that the prevalence of EBV-associated CCA may differ based on anatomic location, which is similar to EBVaGC.[25] In addition, our results demonstrated that EBVaICC was associated with higher HBV infection rate and increased degree of lymphocytic infiltrate; in contrast, EBVaICC had a lower cirrhotic background. Hepatitis B is recognized as a risk factor for ICC.[2,26] It has also been reported that antiviral therapy improves survival in patients with HBV infection and ICC undergoing liver resection.[27,28] These findings presumably show that HBV may have a direct carcinogenic effect or play a synergistic role with EBV on target cells. Chronic liver inflammation resulting from HBV infection may trigger cellular proliferation, which increases the risk of malignant transformation.[29] HBV may act as a co-factor in EBVaICC carcinogenesis, which contributes to tumorigenesis. Both HBV and EBV are highly endemic in southern China, and whether the prevalence of EBVaICC in this region is related to these risk factors needs further study. Of note, although the LEL subtype was significantly related to EBVaICC, more than half of EBVaICC morphologically presented with conventional ICC, which could be underdiagnosed in our routine practices without EBER detection.

The TIME of EBVaICC has not been characterized. In this study, the TIME component was significantly larger in EBVaICC than in nonEBVaICC. These results indicated that the immune response has a closer relationship with EBVaICC than with nonEBVaICC. This immune response could be triggered by EBV harbored in the tumor cells, which resulted in dense lymphocytic infiltrate.[30] Of note, both the size and composition of TIME in EBVaICC were significantly variable among individual cases.

Our results revealed that although the EBV infection did not significantly affect patients' outcome in ICC, the LEL subtype of EBVaICC was significantly related to favorable outcomes. These observations prompted us to analyze the relationship between the characteristics of TIME and patient prognosis. The LEL subtype of EBVaICC had the largest TIME component, and the TIME component was somewhat larger in conventional EBVaICC than in nonEBVaICC. This probably reflects different levels of antitumor immune responses. The conventional type of EBVaICC shared similar TIME features with nonEBVaICC except for significantly increased CD3+ and CD8+ T cell density. Tumor infiltration by B lymphocytes is seldom observed, which may be attributed to the tendency for these cells to rarely migrate outside of lymph nodes.[31] Interestingly, the LEL subtype of EBVaICC, which had a significantly increased density of CD20+ B cells and CD8+ T cells, was significantly related to favorable outcome in ICC. In addition, lymphoid follicular germinal centers were found within these tumors, which indicated an effective humoral immune response in the LEL subtype of EBVaICC. In addition, it has been reported that the close proximity of tumor-infiltrating T cells and B cells indicates a functional interaction between them that is linked to enhanced local immune activation and contributes to better prognosis for patients with HCC.[32] The LEL subtype of EBVaICC was associated with favorable prognostic outcomes, which possibly benefitted from enhanced local immune activation by the significantly increased tumor-infiltrating B cells and CD8+ T cells.

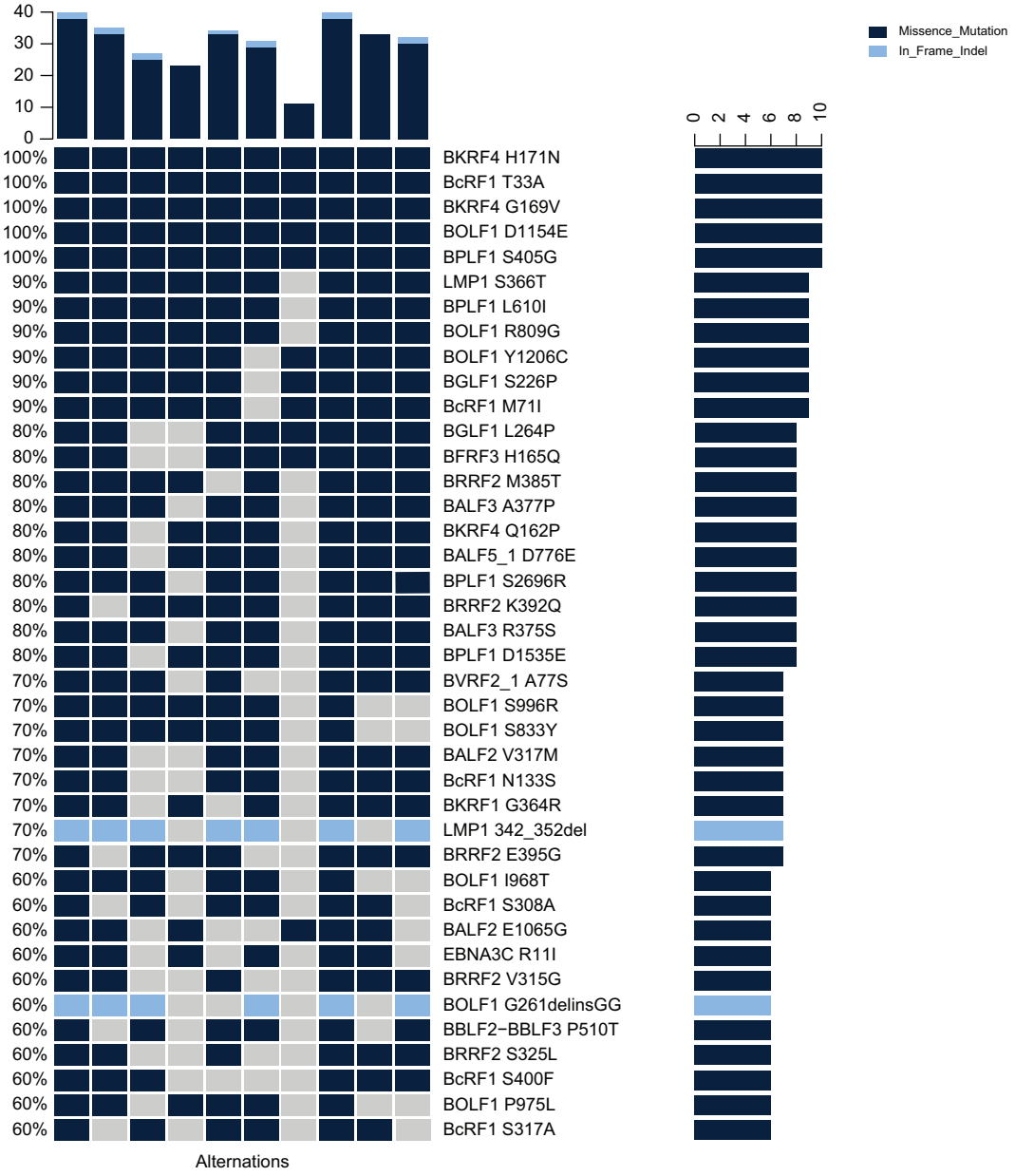

Fig. 8. Nonsynonymous EBV mutations in EBVaICC. The histogram shows the number of top 40 nonsynonymous mutations in ICC-derived EBV, and the mutational heatmap indicates the most recurrent mutations in ICC-derived EBV. EBV, Epstein-Barr virus; EBVaICC, EBV-associated intrahepatic cholangiocarcinoma; ICC, intrahepatic cholangiocarcinoma.

Accordingly, the host immune response is associated with the patient's prognostic outcome rather than the EBV infection status in ICC. The evaluation of histological subtype of EBVaICC is important because it has prognostic significance.

Until recently, the treatment options available to patients with ICC remained limited. Advances in cancer immunology and immunotherapy have facilitated the development of additional treatment options that bring new hope to patients with ICC. The effective selection of suitable cases for immunotherapy will hopefully have a positive impact on advancing toward the goal of developing precision immunotherapy for patients with ICC. Our results revealed significant overexpression of PD-1 and PD-L1 in TILs, and PD-L1 in tumor cells, in EBVaICC. However, the amplification of *CD274* (*PD-L1*), which is an important mechanism of PD-L1 overexpression in EBVaGC,[22] was only identified in 1/20 EBVaICCs by FISH, which suggested the presence of an alternative mechanism of PD-L1 overexpression in EBVaICC. In addition, this study showed that TMIT was significantly related to the EBV infection in ICC. TMIT I (PDL1-Tumor+/CD8^{-High}), which is thought to respond relatively well to checkpoint blockade,[14] was significantly more commonly observed in EBVaICC (90%) than in nonEBVaICC (12.4%). Type I tumors are most likely to benefit from a single agent anti-PD-1/L1 blockade because these tumors have evidence of preexisting intratumor T cells that are turned off by PD-L1 engagement.[14] Therefore, in terms of application, our data suggest that patients with EBVaICC

would be good candidates for immune checkpoint therapy and benefit from anti-PD-1/L1 therapy.

Our study of 10 EBVaICCs using WES revealed the distinct mutational landscape of this rare and special subtype of ICC. We identified a frequent somatic mutation rate and the existence of a high frequency of copy number loss areas. In addition, we discovered 7 frequently mutated genes and 22 significantly mutated potential driver genes and further uncovered several pathways that may contribute to the tumorigenesis of this disease. Of note, none of the reported frequently mutated potential driver genes (*TP53*, *KRAS*, *IDH1*, *PTEN*, *ARID1A*, *EPPK1*, *ECE2* and *FYN*)[15] could be detected in our 10 EBVaICC cases. Interestingly, EBVaICC had a different mutational pattern to LFaCCA[19,20] and HBVaICC,[15] which indicated that a different type of infection-related CCA may have different tumor pathogenesis. We believe that our work provides a valuable starting point for understanding the genetic landscape of mutations in infection-related CCA.

Various EBV strains are differentially distributed throughout the world, and the behavior of cancer-derived EBV strains is different from that of the prototype EBV strain of non-cancerous origin. For the first time, we assembled 10 EBV genomes directly from EBVaICC clinical samples and characterized the mutational landscape of ICC-derived EBV. The single-nucleotide variants of the EBV genome are frequently observed in the *BRLF1*, *BOLF1* and *BRRF2* regions. Of note, new mutation hotspots were observed at *BOLF1* and *BRRF2* in EBVaICC, other than those at *EBNAs*, *LMP1*, *LMP2* and *BDLF2/3* reported in other EBV-associated malignancies.[23,24] All ICC-derived EBV harbored nonsynonymous mutations of *BKRF4* (H171N), *BcRF1* (T33A), *BKRF4* (G169V), *BOLF1* (D1154E) and *BPLF1* (S405G), which were not frequently observed in other EBV-associated tumors. Mutations in *EBNA* loci, which are known as one of the mutational hotspots in EBV-associated tumors, were not commonly observed in ICC-derived EBV. These results indicate that EBV in ICC exhibits unique features in its sequence, which supports the hypothesis of the existence of disease-specific EBV. However, whether the unique EBV is a driver of the development of EBVaICC or simply adapted to the niche of EBVaICC as a bystander requires further investigation.

However, this study is limited in some ways. Although a large cohort of ICC was included, the number of EBVaICC and control groups (pCCA, dCCA and cHCC-CCA) was still small, and some of the results may require verification. Furthermore, due to the poor quality of RNA in fresh tissue specimens, whole transcriptome sequencing failed. In addition, no confident evidence of the integration of the EBV genome was observed based on our WES data. Whole-genome sequencing was not performed, and whether EBV is directly integrated into the host genome is still unknown.

In conclusion, EBVaICC accounted for 6.6% of ICCs in this study, and was associated with EBV latency type I infection and clonal EBV isolates. EBVaICC has unique characteristics regarding clinicopathology, tumor immune microenvironment and molecular genetics. The vast majority of this entity belongs to TMIT I (PD-L1+/CD8^{-High}). Paradoxically, patients could be candidates for immune checkpoint therapy. The LEL subtype of EBVaICC presents an ideal model of host antitumor activity and is significantly related to favorable survival, which may benefit from enhanced local immune activation by tumor-infiltrating B cells and CD8+ T cells.

Abbreviations

CTLA-4, cytotoxic T-lymphocyte-associated protein 4; EBNA1, Epstein-Barr nuclear antigen 1; EBNA2, Epstein-Barr nuclear antigen 2; EBER, Epstein-Barr virus-encoded RNA; EBV, Epstein-Barr virus; EBVaICC, EBV-associated intrahepatic cholangiocarcinoma; EBVaGC, EBV-associated gastric carcinoma; (F) ISH, (fluorescence) *in situ* hybridization; HBVaICC, HBV-associated intrahepatic cholangiocarcinoma; ICC, intrahepatic cholangiocarcinoma; IHC, immunohistochemistical; LEL subtype, lymphoepithelioma-like subtype; LFaCCA, liver fluke-associated cholangiocarcinoma; LFaICC, liver fluke-associated intrahepatic cholangiocarcinoma; LMP1, latent membrane protein 1; NPC, nasopharyngeal carcinoma; OS, overall survival; PD-1, programmed cell death 1; PD-L1, programmed cell death ligand 1; RFS, relapse-free survival; TAMs, tumor-associated macrophages; TILs, tumor-infiltrating lymphocytes; TIME, tumor microenvironment; TMA, tissue microarray; TMIT, tumor environment immune type; WES, whole exon sequencing.

Financial support

This work was supported by the National Key R&D Program of China (2017YFC1309000); the National Natural Science Foundation of China (81872012, 81872266, 81702755, and 81702759); the Natural Science Foundation of Guangdong province (2018B030311005); the Medical Science and Technology Foundation of Guangdong Province (A2018001); and the Natural Science Foundation of Guangdong Province (2018A030313663).

Conflicts of interest

The authors declare no conflicts of interest that pertain to this work.

Please refer to the accompanying ICMJE disclosure forms for further details.

Authors' contributions

Yu-Hua Huang, Chris Zhi-yi Zhang and Qun-Sheng Huang designed the study, analyzed the data, interpreted the results and wrote the manuscript. Joe Yeong, Fang Wang, Xia Yang, Hua Zhang, Yin-Li Zheng and Shi-Lu Chen performed the experiments. Xiao-Long Zhang contributed to bioinformatics analysis. Yang-Fan He, Ru Deng, Cen-Shan Lin and Ming-Ming Yang contributed to clinical and follow-up information collection. Yan Li and Chen Jiang provided support with experimental techniques. Kin-Wah Lee and Stephanie Ma provided supervision and language editing. Mu-Sheng Zeng provided supervision. Jing-Ping Yun conceived the project and provided leadership.

Data availability statement

The data that support the findings of this study are available from the corresponding author upon reasonable request.

Acknowledgements

The authors would like to thank Raybio Medical Technology Limited Co., Guangzhou, China, for providing HALO image analysis software (Indica Labs, v2.3).

Supplementary data

Supplementary data to this article can be found online at https://doi.org/10.1016/j.jhep.2020.10.037.

References

Author names in bold designate shared co-first authorship

[1] Gupta A, Dixon E. Epidemiology and risk factors: intrahepatic cholangiocarcinoma. Hepatobiliary Surg Nutr 2017;6:101–104.
[2] Braconi C, Patel T. Cholangiocarcinoma: new insights into disease pathogenesis and biology. Infect Dis Clin North Am 2010;24:871–884.
[3] Mihalache F, Tantau M, Diaconu B, Acalovschi M. Survival and quality of life of cholangiocarcinoma patients: a prospective study over a 4-year period. J Gastrointestin Liver Dis 2010;19:285–290.
[4] Khan SA, Tavolari S, Brandi G. Cholangiocarcinoma: epidemiology and risk factors. Liver Int 2019;39(Suppl 1):19–31.
[5] Kelley RK, Bridgewater J, Gores GJ, Zhu AX. Systemic therapies for intrahepatic cholangiocarcinoma. J Hepatol 2020;72:353–363.
[6] El-Naggar AK, Chan JK, Grandis JR, Takata T, Slootweg PJ. WHO classification of head and neck tumors. 4th ed. Lyon, France: IARC Press; 2017.
[7] **Qiu MZ**, **He CY**, **Lu SX**, Guan WL, Wang F, Wang XJ, et al. Prospective observation: clinical utility of plasma Epstein-Barr virus DNA load in EBV-associated gastric carcinoma patients. Int J Canc 2020;146:272–280.
[8] Hsu HC, Chen CC, Huang GT, Lee PH. Clonal Epstein-Barr virus associated cholangiocarcinoma with lymphoepithelioma-like component. Hum Pathol 1996;27:848–850.
[9] **Xiao P**, **Shi H**, Zhang H, Meng F, Peng J, Ke Z, et al. Epstein-Barr virus-associated intrahepatic cholangiocarcinoma bearing an intense lymphoplasmacytic infiltration. J Clin Pathol 2012;65:570–573.
[10] Chan AW, Tong JH, Sung MY, Lai PB, To KF. Epstein-Barr virus-associated lymphoepithelioma-like cholangiocarcinoma: a rare variant of intrahepatic cholangiocarcinoma with favorable outcome. Histopathology 2014;65:674–683.
[11] Lin A, Alpert L, Hart J, Chapman C, Pillai AA. Lymphoepithelioma-like carcinomas - a rare variant of cholangiocarcinoma. Hepatology 2020;72:353–355.
[12] Yu MC, Yuan JM. Epidemiology of nasopharyngeal carcinoma. Semin Canc Biol 2002;12:421–429.
[13] Tacyildiz N, Cavdar AO, Ertem U, Oksal A, Kutluay L, Uluoglu O, et al. Unusually high frequency of a 69bp deletion within the carboxy terminus of the LMP-1 oncogene of Epstein-Barr virus detected in Burkitt's lymphoma of Turkish children. Leukemia ;12:1796–1805.
[14] Teng MW, Ngiow SF, Ribas A, Smyth MJ. Classifying cancers based on T-cell infiltration and PD-L1. Canc Res 2015;75:2139–2145.
[15] **Zou S**, **Li J**, **Zhou H**, Frech C, Jiang X, Chu JS, et al. Mutational landscape of intrahepatic cholangiocarcinoma. Nat Commun 2014;5:5696.
[16] Zhang R, Strong MJ, Baddoo M, Lin Z, Wang YP, Flemington EK, et al. Interaction of Epstein-Barr virus genes with human gastric carcinoma transcriptome. Oncotarget 2017;13:38399–38412.
[17] Lin DC, Meng X, Hazawa M, Nagata Y, Varela AM, Xu L, et al. The genomic landscape of nasopharyngeal carcinoma. Nat Genet 2014;46:866–871.
[18] Hong S, Liu D, Luo S, Fang W, Zhan J, Fu S, et al. The genomic landscape of Epstein-Barr virus-associated pulmonary lymphoepithelioma-like carcinoma. Nat Commun 2019;10:3108.
[19] Ong CK, Subimerb C, Pairojkul C, Wongkham S, Cutcutache I, Yu W, et al. Exome sequencing of liver fluke-associated cholangiocarcinoma. Nat Genet 2012;44:690–693.
[20] Chan-On W, Nairismagi ML, Ong CK, Lim WK, Dima S, Pairojkul C, et al. Exome sequencing identifies distinct mutational patterns in liver fluke-related and non-infection-related bile duct cancers. Nat Genet 2013;45:1474–1478.
[21] Masson E, Chen JM, Cooper DN, Ferec C. PRSS1 copy number variants and promoter polymorphisms in pancreatitis: common pathogenetic mechanism, different genetic effects. Gut 2018;67:592–593.
[22] The Cancer Genome Atlas Research Network. Comprehensive molecular characterization of gastric adenocarcinoma. Nature 2014;513:202–209.
[23] Palser AL, Grayson NE, White RE, Corton C, Correia S, Ba Abdullah MM, et al. Genome diversity of Epstein-Barr virus from multiple tumor types and normal infection. J Virol 2015;89:5222–5237.
[24] **Peng RJ**, **Han BW**, **Cai QQ**, Zuo XY, Xia T, Chen JR, et al. Genomic and transcriptomic landscapes of Epstein-Barr virus in extranodal natural killer T-cell lymphoma. Leukemia 2019;33:1451–1462.
[25] Murphy G, Pfeiffer R, Camargo MC, Rabkin CS. Meta-analysis shows that prevalence of Epstein-Barr virus-positive gastric cancer differs based on sex and anatomic location. Gastroenterology 2009;137:824–833.
[26] Zhang H, Zhu B, Zhang H, Liang J, Zeng W. HBV infection status and the risk of cholangiocarcinoma in Asia: a meta-analysis. Biomed Res Int 2016;2016:3417976.
[27] **Lei Z**, **Xia Y**, **Si A**, Wang K, Li J, Yan Z, et al. Antiviral therapy improves survival in patients with HBV infection and intrahepatic cholangiocarcinoma undergoing liver resection. J Hepatol 2018;68:655–662.
[28] **Sha M**, **Jeong S**, Xia Q. Antiviral therapy improves survival in patients with HBV infection and intrahepatic cholangiocarcinoma undergoing liver resection: novel concerns. J Hepatol 2018;68:1315–1316.
[29] Ralphs S, Khan SA. The role of the hepatitis viruses in cholangiocarcinoma. J Viral Hepat 2013;20:297–305.
[30] Song HJ, Srivastava A, Lee J, Kim YS, Kim KM, Ki Kang W, et al. Host inflammatory response predicts survival of patients with Epstein-Barr virus-associated gastric carcinoma. Gastroenterology 2010;139:84–92.
[31] Goeppert B, Frauenschuh L, Zucknick M, Stenzinger A, Andrulis M, Klauschen F, et al. Prognostic impact of tumor-infiltrating immune cells on biliary tract cancer. Br J Canc 2013;109:2665–2674.
[32] Garnelo M, Tan A, Her Z, Yeong J, Lim CJ, Chen J, et al. Interaction between tumor-infiltrating B cells and T cells controls the progression of hepatocellular carcinoma. Gut 2017;66:342–351.